

## Energy-loss near-edge structure changes with bond length in carbon systems

J. T. Titantah and D. Lamoen

*TSM, Departement Fysica, Universiteit Antwerpen, Groenenborgerlaan 171, 2020 Antwerpen, Belgium*

(Received 18 April 2005; revised manuscript received 22 July 2005; published 23 November 2005)

We show that when the graphene planes of graphite are uniformly expanded, thereby increasing the C—C bond length to 1.7 Å, the  $\sigma^*$  edge onset of the energy-loss near-edge structure (ELNES) spectrum shifts to lower energies by almost 5 eV, meanwhile the  $\pi^*$  edge shifts by less than 0.2 eV. The shift of the  $\sigma^*$  edge demonstrates that for bond lengths which are typical of some carbon systems such as amorphous carbon, it is possible to find  $\sigma^*$  features in the ELNES spectra at energies as low as 286–288 eV. Calculations on 64-atom amorphous carbon (*a*-C) and amorphous carbon nitride model structures characterized by a wide range of bond lengths confirm this. Most of the  $sp^2/sp^3$  quantification techniques that are available overlook this issue of  $\sigma^*$  contamination of the  $\pi^*$  region and assume that all features within this energy range are entirely of  $\pi^*$  origin. We show that the effect of bond length variation on the  $\pi^*$  spectrum of graphite and *a*-C is minor, thereby supporting the reliability of the former spectrum for  $sp^2/sp^3$  quantification purposes, as was recently demonstrated [see J. T. Titantah and D. Lamoen, Phys. Rev. B **70**, 075115 (2004)].

DOI: [10.1103/PhysRevB.72.193104](https://doi.org/10.1103/PhysRevB.72.193104)

PACS number(s): 79.20.Uv, 71.15.Mb, 78.70.Dm, 71.15.Qe

The mechanical, optical, and electronic properties of amorphous carbon (*a*-C) depend strongly on the short-range environment of the atoms. The local structure of the carbon atoms varies between the  $sp^2$ -like graphitic bonding state and the  $sp^3$ -like diamond bonding state. Therefore, it is important to determine quantitatively the  $sp^2/sp^3$  ratio in amorphous carbon systems. Electron energy-loss spectroscopy (EELS) and x-ray absorption spectroscopy (XAS) are among the most reliable techniques to quantify the  $sp^2/sp^3$  ratio. The  $sp^3$  fraction is obtained from an analysis of the  $\pi^*$ - and  $\sigma^*$ -related features of the energy-loss near-edge structure (ELNES) and x-ray absorption near-edge structure (XANES). For both techniques the energy range of 284–295 eV is important with the  $\pi^*$  and  $\sigma^*$  peaks located at about 285 and 291 eV, respectively.

There has been some speculation on the origin of the 287–288 eV feature (found between the well-known  $\pi^*$  and  $\sigma^*$  peaks) that is often observed in the ELNES spectra of *a*-C materials. It is often said to originate from the  $1s \rightarrow \pi^*$  transition for  $sp^2$  carbon atoms bonded to hydrogen<sup>1</sup> or from carbon atoms in an intermediate state.<sup>2</sup> Both suggestions assume all features within this energy range to be entirely of  $\pi^*$  character and this should influence the results of the  $sp^2/sp^3$  characterization of amorphous carbon materials. Using a plane wave density functional theory code on a 16 atom supercell, Pickard<sup>3</sup> reported a peak at about 3 eV above the edge onset (287–288 eV) in the *K* edge of carbon for graphite and attributed it to interlayer states. Recent calculations by our group<sup>4,5</sup> showed a similar feature. Several features have also been reported in the XANES and ELNES of amorphous carbon nitride (*a*-CN<sub>x</sub>) systems within the energy range of 286–290 eV,<sup>6</sup> but the assignment of the origin of these peaks is still a topic of debate. Following the assignment of Ref. 7, the authors of Ref. 6 attributed the feature at about 289 eV to the  $\sigma^*$  transition of the C—H bonds.

In this work we present calculations of the energy-loss near-edge structure of graphite in 36 and 64 atom supercells, respectively, and that of diamond within a 64-atom supercell.

We show that the  $\sigma^*$  edge is very sensitive to the C—C bond length, in agreement with x-ray absorption measurements on C<sub>6</sub>H<sub>6</sub> and C<sub>6</sub>H<sub>12</sub>.<sup>8</sup> We also show that the feature reported by Pickard is a consequence of the core-core interaction resulting from the use of a small supercell size. ELNES calculations are also presented for *a*-C and *a*-CN<sub>x</sub> systems. The *a*-C system contains 64 atoms at a density of 2.8 g/cm<sup>3</sup>, while the *a*-CN<sub>x</sub> is made of 10 nitrogen atoms in a 54-atom amorphous carbon matrix at a density of 2.1 g/cm<sup>3</sup>. The amorphous structures are generated as follows. Using the Tersoff empirical potential for carbon<sup>9</sup> with periodic boundary conditions we quench liquid carbon from a temperature of about 5000 to 300 K. The resulting structure is then relaxed further using density functional theory (DFT) techniques.<sup>10</sup> For the *a*-CN<sub>x</sub>, 10 atoms are selected from the 64 atoms and replaced by nitrogen, and the resulting system is relaxed further using the DFT technique.

DFT calculations are performed on graphite (with hexagonal lattice parameters of 2.46 and 6.70 Å) and diamond (with face-centered-cubic lattice parameters of 3.57 Å). Supercells in which the lattice parameters are rescaled to yield specific bond lengths are used. We make use of the all-electron full-potential-(linearized)-augmented-plane-wave+local orbital code WIEN2K,<sup>10</sup> in which the exchange-correlation potential is treated within the local density approximation.<sup>11</sup> Twenty and 40 *k* points in the irreducible Brillouin zone are used for the self-consistent field (SCF) calculations of diamond and graphite, respectively, while for the *a*-C and the *a*-CN<sub>x</sub> 32 *k* points were used for the SCF calculations. The muffin-tin radii  $R_M$  are set at 1.3 atomic units (a.u.) for graphite and diamond and 1.1 a.u. for *a*-C and *a*-CN<sub>x</sub>. The interstitial plane-wave vector cutoff  $k_M$  is chosen such that  $R_M \times k_M = 5.5$  for graphite and diamond and 4.5 for *a*-C and *a*-CN<sub>x</sub>. ELNES spectra are calculated using the formulation of Nelhiebel *et al.*<sup>12</sup> as implemented in the WIEN2K code. This formulation allows an easy separation of the ELNES of graphite into the  $\pi^*$  and  $\sigma^*$  components. In all the systems considered, the core-hole effect is accounted for via the excited core method, whereby the electron occupancy of the

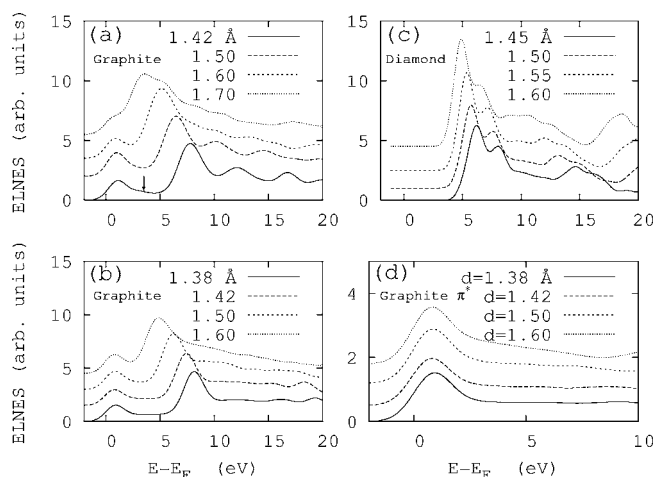


FIG. 1. Calculated ELNES spectra of (a) graphite for the  $3 \times 3 \times 1$  supercell, (b) graphite for the  $4 \times 4 \times 1$  supercell, and (c) diamond for the  $2 \times 2 \times 2$  supercell. (d) The graphite  $\pi^*$  ELNES spectrum for the  $4 \times 4 \times 1$  supercell.  $E_F$  denotes the Fermi level. Lattice parameters are rescaled to yield the indicated bond lengths.

core state is reduced by one while charge neutrality is ensured by the introduction of a uniform background charge. This means that for both the  $a$ -C and the  $a$ -CN<sub>x</sub> systems 64 calculations were performed. For all the ELNES calculations we adopted the so-called magic convergence and collection semiangles of 1.87 and 3.01 mrad, respectively.<sup>13</sup>

In Fig. 1(a) the total ELNES spectrum of graphite obtained with a  $3 \times 3 \times 1$  supercell is shown for a series of C—C bond lengths. This system size is larger than that used by Pickard<sup>3</sup> and the effect of a remnant core-core interaction (due to the periodic boundary conditions) on the ELNES spectrum can be seen in the form of a shoulder on the higher-energy side of the main  $\pi^*$  peak, as indicated by the arrow. This shoulder vanishes for the  $4 \times 4 \times 1$  supercell used to get the result in Fig. 1(b). Irrespective of the supercell size used, it is clearly seen that while the  $\pi^*$  edge is less sensitive to the C—C bond length (a maximum of 0.2 eV was recorded), the  $\sigma^*$  edge shifts to lower energy as the bond length increases. Calculations on diamond [shown in Fig. 1(c)] show that a similar trend is observed for the latter, but the sensitivity is weaker than for graphite or aromatic hydrocarbon systems.<sup>8</sup> For example, when the C—C bond length in graphite is changed from 1.38 to 1.60 Å the  $\sigma^*$  edge position moves from 8.2 to 4.9 eV, but when the bond length in diamond is increased from 1.40 to 1.60 Å the  $\sigma^*$  edge position moves from 6.6 to 5.0 eV.

The  $\pi^*$  ELNES spectra of graphite were calculated from an orientation resolved calculation<sup>4,13</sup> and are plotted in Fig. 1(c). It follows from this figure that the  $\pi^*$  spectrum is very weakly affected by the bond length variations.

In order to investigate the effect of bond length variation on the ELNES spectrum of amorphous carbon materials we show in Fig. 2 the average (over all carbon atoms) ELNES spectrum of the  $a$ -C structure at a density of 2.8 g/cm<sup>3</sup> and of an  $a$ -CN<sub>x</sub> system made of 16 at. % nitrogen at a density of 2.1 g/cm<sup>3</sup>. In Fig. 2 we also show the ELNES spectrum of two representative carbon atoms: a threefold-coordinated

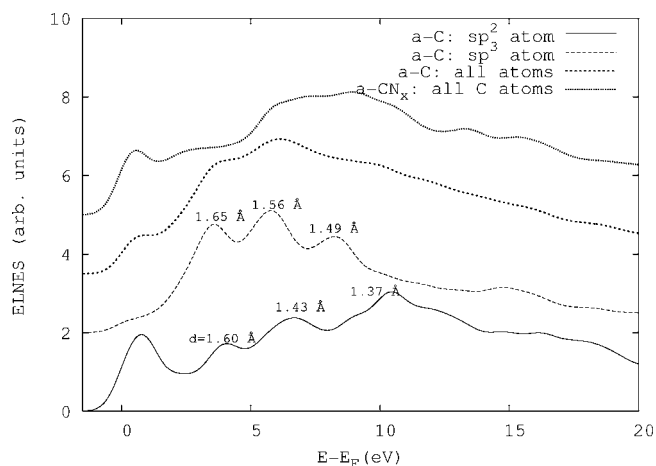


FIG. 2. Calculated ELNES spectrum of amorphous carbon and amorphous carbon nitride systems: The spectra for typical “ $sp^2$ ” and “ $sp^3$ ” atoms, each bonded to carbon atoms with varying bond lengths are also shown and the fine structures are correlated to the various bond lengths. The total ELNES spectrum of the  $a$ -C system shows two fine structures at the  $\sigma^*$  edge, demonstrating the bond length distribution in the system.

(“ $sp^2$ ”) and a fourfold-coordinated (“ $sp^3$ ”) atom. The coordination number of an atom was defined as the number of atoms sitting within a sphere of radius 1.9 Å centered on this atom. For the densities at which simulations were done only threefold- and fourfold-coordinated atoms were found. In the spectra of the two atoms the fine structures can be correlated with the various bond lengths associated with each atom. Basically three types of bonds were isolated for both atoms. For the “ $sp^2$ ” atom bond lengths of 1.37, 1.43, and 1.60 Å were found and correlated with the three features at about 9, 7, and 4 eV above the Fermi level, respectively. This assignment was guided by the results on graphite and diamond. The “ $sp^3$ ” atom had four bonds of which one had a length of 1.49 Å, two had bond lengths of 1.56 Å and the fourth had a length of 1.65 Å. We would like to point out that all our simulated amorphous carbon structures show this behavior, namely, all four-coordinated atoms were characterized by a short bond ( $\leq 1.5$  Å), two intermediate bonds ( $\sim 1.55$  Å) and a long bond ( $\geq 1.6$  Å). The three features at 8.5, 6, and 3.5 eV in the ELNES spectrum of this atom correspond, respectively, to these three bond types. The ELNES spectrum of the atoms of the  $a$ -CN<sub>x</sub> system also showed a similar trend, in particular a more drastic effect was recorded as shown on the topmost graph of Fig. 2. The ELNES spectrum was now composed of three major features: the usual  $\pi^*$  peak, a  $\sigma^*$  feature beyond 5 eV, and a broad feature intermediate between them. This feature, which looks similar to that reported in Ref. 6 is correlated to transitions linked to various C—N  $\sigma$  bonds, in contrast to the assignment to C—H  $\sigma$  bonds of Lee *et al.*<sup>7</sup> A detailed study of the structural and electronic properties of the  $a$ -CN<sub>x</sub> will be presented elsewhere. We calculated the bond lengths for every carbon atom in the  $a$ -C and  $a$ -CN<sub>x</sub> structures and assigned the features in the ELNES spectrum of each atom to particular bond lengths that characterize the atom. In Fig. 3 we give the energies of the various peaks for a representative set of “ $sp^2$ ” atoms,

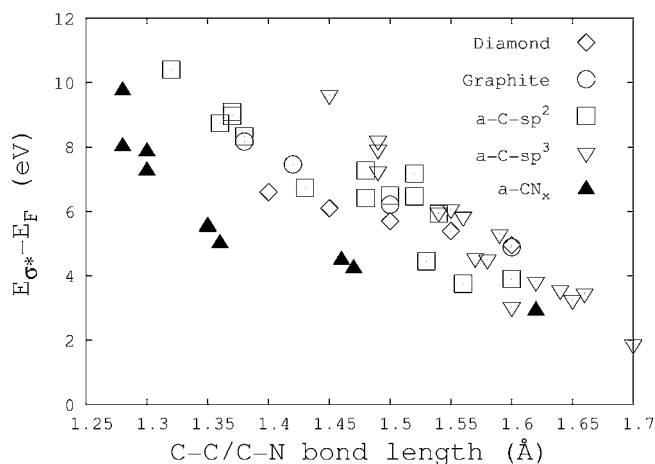


FIG. 3. The energy of the  $\sigma^*$  edge with respect to the Fermi level as a function of bond length. Results are presented for diamond, graphite and some atoms within amorphous carbon and amorphous carbon nitride matrices. The atoms within the  $a$ -C matrix are grouped into  $sp^2$ - and  $sp^3$ -hybridized atoms.

“ $sp^3$ ” atoms, and carbon atoms bonded to nitrogen in  $a$ - $CN_x$ . The atoms were chosen to span the relevant range of bond lengths for  $a$ -C and  $a$ - $CN_x$ . Shown on the figure are also the results for graphite and diamond with the rescaled bond lengths. The general trend for all the carbon materials considered is that as the bond length grows, the  $\sigma^*$  edge shifts to lower energies, and the shift is more pronounced for  $a$ - $CN_x$  systems. Figure 2 shows that depending on the bond length the position of the  $\sigma^*$  edge can vary from about 295 eV (11 eV above the Fermi level) for a bond length of about 1.35 Å to 287 eV (3 eV above the Fermi level) for a bond length of about 1.7 Å. In  $a$ -C bond lengths easily vary from 1.3 to 1.7 Å. Such a wide distribution of bond length is likely the reason for the broad distribution of the  $\sigma^*$  edge, which can overlap with the  $\pi^*$  peak, making the latter show up only as a shoulder.<sup>14,15</sup> This is often the case for highly tetrahedral amorphous carbon, especially when the few “ $sp^2$ ” atoms are highly dispersed throughout the film (not clustered together) and the bond lengths are longer than the equilibrium  $C_{sp^2}$ - $C_{sp^2}$  bond length in graphite. The sharp nature of the  $\pi^*$  peak in some  $sp^2$ -rich amorphous carbon systems can be understood from the weak dependence of the  $\pi^*$  spectrum on the bond length.

As pointed out in the introduction, the energy range of

284–295 eV is important for the  $sp^2/sp^3$  quantification of carbon systems. For binary systems, for example, amorphous carbon nitrides, hydrogenated amorphous carbon, or ternary systems such as boron-carbon-nitride composites, the bonding structure becomes complicated. In such cases the accuracy of the ELNES and XANES based techniques will depend crucially on how efficient the  $\pi^*$  and  $\sigma^*$  features are treated. Because of this the fixed energy window<sup>16</sup> and the functional fitting<sup>2,17</sup> methods may suffer adversely from the  $\sigma^*$  contamination of the  $\pi^*$  intensity. The consequence of this will be an underestimation of the fraction of  $sp^3$ -bonded carbon in the system. To solve this problem we recently proposed a method of  $sp^2/sp^3$  quantification of carbon materials based on the theoretical  $\pi^*$  ELNES spectrum of graphite.<sup>4,5</sup> The main assumption of the method was that apart from a disorder-induced broadening, the ELNES of a carbon atom sitting in an  $sp^2$  environment should be similar to that of graphite. This assumption was supported by calculations of the  $\pi^*$  ELNES spectrum of  $sp^2$  atoms in an amorphous carbon matrix. The near invariance of the  $\pi^*$  ELNES spectrum of graphite with bond length variation gives further credibility to this assumption, thereby confirming the reliability of the technique for bonding characterization of carbon-based materials.

In summary, we have calculated the energy-loss near-edge structure of carbon in graphite, diamond, amorphous carbon, and amorphous carbon nitride structures with lattice parameters of graphite and diamond rescaled to span a wide range of relevant bond lengths. The  $\sigma^*$  edge is found to depend on the bond lengths and the hybridization state of the atom. Longer bonds tend to contribute to the lower energy part of the  $\sigma^*$  spectrum. It is found that when carbon is bonded to a foreign atom like nitrogen the shift to lower energies can be drastic, resulting in an entirely different energy loss near-edge structure, or near-edge x-ray absorption fine structure, at energies intermediate between the main  $\pi^*$  and  $\sigma^*$  features. We have thus shown that the  $\sigma^*$  edge of carbon can be used as a probe of bond length distribution in carbon materials. The consequence of a large spread of bond length is evidenced in the ELNES as a broad  $\sigma^*$  edge with edge energies overlapping with regions of the spectrum that are known to characterize  $\pi^*$  features. This also implies that any technique aimed at quantifying the  $sp^2/sp^3$  fraction in amorphous carbon systems should account for this effect. The method developed by the authors in Ref. 4 correctly treats this  $\sigma^*$  contamination of the  $\pi^*$  peak.

<sup>1</sup>S. R. P. Silva, J. Robertson, Rusli, G. A. J. Amaratunga, and J. Schwan, *Philos. Mag. B* **74**, 369 (1996).

<sup>2</sup>A. J. Papworth, C. J. Kiely, A. P. Burden, S. R. P. Silva, and G. A. J. Amaratunga, *Phys. Rev. B* **62**, 12 628 (2000).

<sup>3</sup>C. J. Pickard, Ph.D. thesis, Cambridge University, Cambridge, U.K., 1997, p. 94.

<sup>4</sup>J. T. Titantah and D. Lamoen, *Phys. Rev. B* **70**, 075115 (2004).

<sup>5</sup>J. T. Titantah and D. Lamoen, *Carbon* **43**, 1311 (2005).

<sup>6</sup>R. McCann, S. S. Roy, P. Papakonstantinou, I Ahmad, P. Magu-

ire, J. A. MacLaughlin, L. Petaccia, S. Lizzit, and A. Goldoni, *Diamond Relat. Mater.* **14**, 2005 (2005).

<sup>7</sup>C. S. Lee, J. K. Shin, K. Yong Eun, K. R. Lee, and K. H. Yoon, *J. Appl. Phys.* **95**, 4829 (2004).

<sup>8</sup>G. Comelli, J. Stöhr, C. J. Robinson, and W. Jark, *Phys. Rev. B* **38**, 7511 (1988).

<sup>9</sup>J. Tersoff, *Phys. Rev. B* **38**, 9902 (1988).

<sup>10</sup>P. Blaha, K. Schwarz, G. K. H. Madsen, D. Kvasnicka, and J. Luitz, *WIEN2k, An Augmented Plane Wave+Local Orbitals*

- Program for Calculating Crystal Properties* (Karlheinz Schwarz, Technische Universität Wien, 2001).
- <sup>11</sup>J. P. Perdew and Y. Wang, Phys. Rev. B **45**, 13 244 (1992).
- <sup>12</sup>M. Nelhiebel, P. H. Louf, P. Schattschneider, P. Blaha, K. Schwarz, and B. Jouffrey, Phys. Rev. B **59**, 12 807 (1999).
- <sup>13</sup>J. T. Titantah, K. Jorissen, and D. Lamoen, Phys. Rev. B **69**, 125406 (2004).
- <sup>14</sup>T. A. Friedmann, J. P. Sullivan, J. A. Knapp, D. R. Tallant, D. M. Follstaedt, D. L. Medlin, and P. B. Mirkarimi, Appl. Phys. Lett. **71**, 3820 (1997).
- <sup>15</sup>D. G. McCulloch, J. L. Peng, D. R. McKenzie, S. P. Lau, D. Sheeja, and B. K. Tay, Phys. Rev. B **70**, 085406 (2004).
- <sup>16</sup>S. D. Berger, D. R. McKenzie, and P. J. Martin, Philos. Mag. Lett. **57**, 285 1988.
- <sup>17</sup>L. Wan and R. F. Egerton, Thin Solid Films **279**, 34 1996.